Synergistic Interactions between Activated Carbon Fabrics and Toxic Hexavalent Chromium

Cuixia Xu,[a,b] Bin Qiu,[a,c] Hongbo Gu,[a] Xingru Yang,[a] Huige Wei,[a] Xiaohua Huang,[d] Yiran Wang,[a] Dan Rutman,[a] Dongmei Cao,[e] Saheel Bhana,[d] Zhanhu Guo,[a,*,z] and Suying Wei[a,b,z]

[a]*Integrated Composites Lab (ICL), Dan F. Smith Department of Chemical Engineering, Lamar University, Beaumont, Texas 77710, USA*
[b]*Department of Chemistry and Biochemistry, Lamar University, Beaumont, Texas 77710, USA*
[c]*College of Environmental Science and Engineering, Beijing Forestry University, Beijing 100083, China*
[d]*Department of Chemistry, The University of Memphis, Memphis, Tennessee 38152, USA*
[e]*Material Characterization Center, Louisiana State University, Louisiana 70803, USA*

The synergistic interactions between the activated carbon fabrics (ACFs) and the toxic Cr(VI) were investigated aiming to functionalize the ACFs and to remove the toxic Cr(VI). The effects of pH, treatment time, initial Cr(VI) concentration and ACFs dose on the Cr(VI) removal were studied. Different pH values had different effects on the Cr(VI) removal by ACFs, pH = 1.0 was found to be the optimum. For the pH = 1.0 solution, the Cr(VI) in the aqueous solution was reduced to Cr(III) and adsorbed onto the ACFs, and the C-O and C=O functional groups were found on the ACFs surface. The redox kinetic in the pH = 1.0 solution could be described by the pseudo-first-order model and the typical value of the pseudo-first-order rate constant was calculated to be 0.0872 min^{-1}. Langmuir, Freundlich, and Temkin adsorption isotherm models were applied to describe isotherm behaviors. The Cr(VI) equilibrium data agreed well with the Langmiur isotherm model with a maximum adsorption capacity of 5.59 mg g^{-1}. The ACFs could be easily regenerated by 1.0 mol L^{-1} sodium hydroxide and effectively recycled 7 times with the removal percentage decreased by 16.5%, which was caused by the irreversible formation of oxygen functional groups on the surface of ACFs.
© 2013 The Electrochemical Society. [DOI: 10.1149/2.004403jss] All rights reserved.

Hexavalent chromium, one of the main pollutants, has been widely used in various industries including electroplating,[1] leather tanning,[2] metal finishing[3] and mining.[4] Chromium can cause severe environmental and public health problems. The US Environmental Protection Agency (EPA) has classified chromium as Group A carcinogen and allows a maximum contaminant level (MCL) of 100 μg L^{-1} for total chromium according to the national primary drinking water regulations.[5,6] Chromium exists in the environment mainly in two states: Cr(III) and Cr(VI). Cr(III) is an essential element in humans and is much less toxic than Cr(VI). Cr(VI) is highly soluble and mobile, primarily presented in the form of chromate (CrO_4^{2-}) and dichromate ($Cr_2O_7^{2-}$) ions.[7,8] Due to the health hazards of Cr(VI), numerous studies concerning its removal from aqueous solutions have been performed using different processes, including cyanide treatment,[9] electro-chemical precipitation,[10] ion exchange,[11] and adsorption.[12–16] Among all of them, adsorption is a versatile method for metal removal including Cr(VI) due to its low operation cost and short operation time without secondary toxic compounds.[17,18]

Activated carbons are of common use in many advanced environmental applications, such as, purification,[19] decolorization,[20,21] depollution,[22] deodorization,[23] and metal adsorption.[24] They have various forms: grains, powders and fibers. Fibers can be arranged to packed beds or be glued together using various binder systems. ACFs making of carbon fibers exhibit strong mechanical properties, impressive thermal stability, and good resistance to solvents and acids. Compared to granular or powdered adsorbents, they have higher specific surface areas (>1000 m² g^{-1}) and faster kinetics of adsorption with easiness of regenerative use.[25] ACFs can additionally be folded and mounted on frames to fit in various systems, holding forth the promise of extensive use in many respects.[26,27] Even though various available adsorbents like activated carbons,[9,27,28] sawdusts,[29] cyanobacteriums[30] and baggasse fly ashes[31] have been reported to remove hazardous heavy metals, most of them have a low Cr(VI) adsorption capacity.[32] Compared with others, ACFs have been investigated as promising adsorbents for removing heavy metals,[33] as they can be easily modified by chemical treatments to increase their properties, easy to be operated and recycled. Though the Cr(VI) adsorption behaviors of the ACFs have been explored for Cu(II), Ni(II), Pb(II) and Cr(VI),[34]

the mechanism of the adsorption of ACFs and synergistic interactions between ACFs and heavy metal were unfortunately rarely reported. To understand the surface functionalities of the ACFs will help the design of functional polymer nanocomposites, where the interfacial bonding and compatibility with the hosting polymer matrix will be very critically important.

In this paper, the synergistic interactions between the as-received ACFs and the toxic Cr(VI) is explored. The effects of pH value, treatment time, initial Cr(VI) concentration and ACFs dose on these synergies have been studied. The surface functionalities of the ACFs after treated with the Cr(VI) solutions with different pH values for different treatment time have been systematically studied by X-ray photoelectron spectroscopy (XPS), thermogravimetric analysis (TGA), Raman spectroscopy, scanning electron microscopy (SEM) and Energy dispersive spectroscopy (EDS). The kinetic and adsorption isotherm behaviors of the as-received ACFs in the Cr(VI) solution with a pH value of 1.0 have been investigated. And the regeneration of as-received ACFs has been reported as well.

Experimental

Materials.— Activated carbon fabrics (1500 m² g^{-1}) were purchased from American Technical Trading, Inc. ACFs were washed with deionized water and dried at 50°C in vacuum oven overnight before usage. Potassium dichromate ($K_2Cr_2O_7$) and 1,5-diphenylcarbazide (DPC) were purchased from Alfa Aesar Company. Phosphoric acid (H_3PO_4, 85 wt%), acetone, nitric acid (68.0–70.0%), sodium hydroxide and sulfuric acid (98%) were obtained from Fisher Scientific. Ammonium persulfate (APS, $(NH_4)_2S_2O_8$) was purchased from Sigma Aldrich. All the chemicals were used as-received without any further treatment.

Synergistic interactions between Cr(VI) and ACFs under different conditions.— The pH value effect on the Cr(VI) removal ACFs was investigated by selecting Cr(VI) solutions with a pH value of 1.0, 2.0, 4.0, 8.0 and 10.0, respectively. The initial pH value of Cr(VI) solution was adjusted by NaOH (1.0 mol L^{-1}) and HCl (1.0 mol L^{-1}) with a pH meter (Vernier LabQuest with pH-BTA sensor). The pH = 1.0 Cr(VI) solution was adjusted by concentrated sulfuric acid. The ACFs (40.0 mg) were ultrasonically (Branson 8510) treated in 50.0 mL

*Electrochemical Society Active Member.
zE-mail: suying.wei@lamar.edu; zhanhu.guo@lamar.edu

certain pH value of Cr(VI) solution (1000 µg L^{-1}) for 30 min. Then this solution was taken out for Cr(VI) concentration determination.

The effect of ACFs dose on the Cr(VI) removal was studied by using ACFs with a loading from 0.1 to 0.8 g L^{-1} to treat 50.0 mL Cr(VI) solution with a Cr(VI) concentration of 1000 µg L^{-1} at pH = 1.0 for 30 min.

The effect of initial Cr(VI) concentration on the Cr(VI) removal was investigated by using ACFs (40.0 mg) to treat Cr(VI) solutions (50.0 mL, pH = 1.0) with Cr(VI) concentration varying from 1000 to 4000 µg L^{-1} for 30 min.

For kinetic study, the ACFs (50.0 mg) were carried out to treat 80.0 mL Cr(VI) solution with an initial Cr(VI) concentration of 1000 µg L^{-1} at pH = 1.0 for different treatment periods. The Cr(VI) removal tests were all conducted at room temperature.

The adsorption-desorption cycles were carried out as follows: (a) adsorption experiment: the ACFs (40.0 mg) were ultrasonically treated in 50.0 mL Cr(VI) solution (1000 µg L^{-1}, pH = 1.0) for 30 min; and (b) desorption experiment: the ACFs after adsorption were ultrasonically treated with 10 mL 0.1 mol L^{-1} NaOH solution over a period time of 10 min.

The final concentration of Cr(VI) was determined by colorimetric method.[35] For colorimetric analysis, the chromium solution (5.25 mL) was taken into test tube, o-phosphoric acid (0.50 mL, 4.5 M) and DPC acetone solution (0.25 mL, 5 g L^{-1}) were added. After incubated at room temperature for 30 min for color development, the absorbance of the sample was measured in a UV-vis spectrophotometer (Cary 50). The obtained standard fitting equation was $A = 9.7232 \times 10^{-4} C$; where C is the concentration of Cr(VI), A is the absorbance at 540 nm wavelength obtained from the UV-vis spectrophotometer.

The Cr(VI) removal percentage ($R\%$) is calculated using Equation 1:

$$R\% = \frac{C_0 - C_e}{C_0} \times 100\% \qquad [1]$$

where C_0 (µg L^{-1}) is the initial Cr(VI) concentration and C_e (µg L^{-1}) is the final Cr(VI) concentration in solution after treatment.

Characterization.— The morphologies of the ACFs samples were observed with JEOL field emission scanning electron microscope (JSM-6700F system). The EDS attached to the SEM was used to characterize the elemental component for both the fresh and treated ACFs.

The thermal stability of the ACFs and the ACFs samples after treated with Cr(VI) solution was conducted in a thermo-gravimetric analysis (TGA, TA instruments, Q-500) with a heating rate of 10°C min^{-1} under an air flow rate of 60 mL min^{-1} from 30 to 800°C.

The X-ray photoelectron spectroscopy (XPS) measurements were performed in the Kratos AXIS 165 XPS/AES instrument using a monochromatic Al K radiation to see the elemental compositions. The C1s and Cr2p peaks were deconvoluted into the components consisting of a Gaussian line shape Lorentzian function (Gaussian = 80%, Lorentzian = 20%) on Shirley background.

Raman spectra were obtained using a Horiba Join-Yvon LabRam Raman confocal microscope with 785 nm laser excitation at a 1.5 cm^{-1} resolution at room temperature.

Results and Discussion

Interaction between the ACFs and Cr(VI).— Fig. 1 shows the SEM microstructure and the EDS elemental analysis of the ACFs and the ACFs samples treated with 1000 µg L^{-1} Cr(VI) solution (pH = 1.0), 1000 µg L^{-1} (pH = 7.0) Cr(VI) solution and 2 g L^{-1} Cr(VI) solution (pH = 1.0) for 30 min. Compared to the pure carbon element in the as-received ACFs in Fig. 1A inset, the oxygen element is observed in ACFs samples treated with Cr(VI) solution, Fig. 1B–1D inset, indicating that the ACFs have been oxidized by Cr(VI) solution and some oxygen functional groups are introduced to the ACFs. In addition, the Cr element is detected in the ACFs sample treated with concentrated Cr(VI) solution of 2 g L^{-1}. For the ACFs samples treated with 1000 µg L^{-1} Cr(VI) solution in Fig. 1B & 1C, the amount of chromium on the ACFs is below the limit of EDS detection. From the SEM images, the surface of the as-received ACFs is very smooth in Fig. 1A, the diameter of the carbon fibers that make the ACFs is very uniform. After treatment in pH = 1.0 and pH = 7.0 Cr(VI) solution
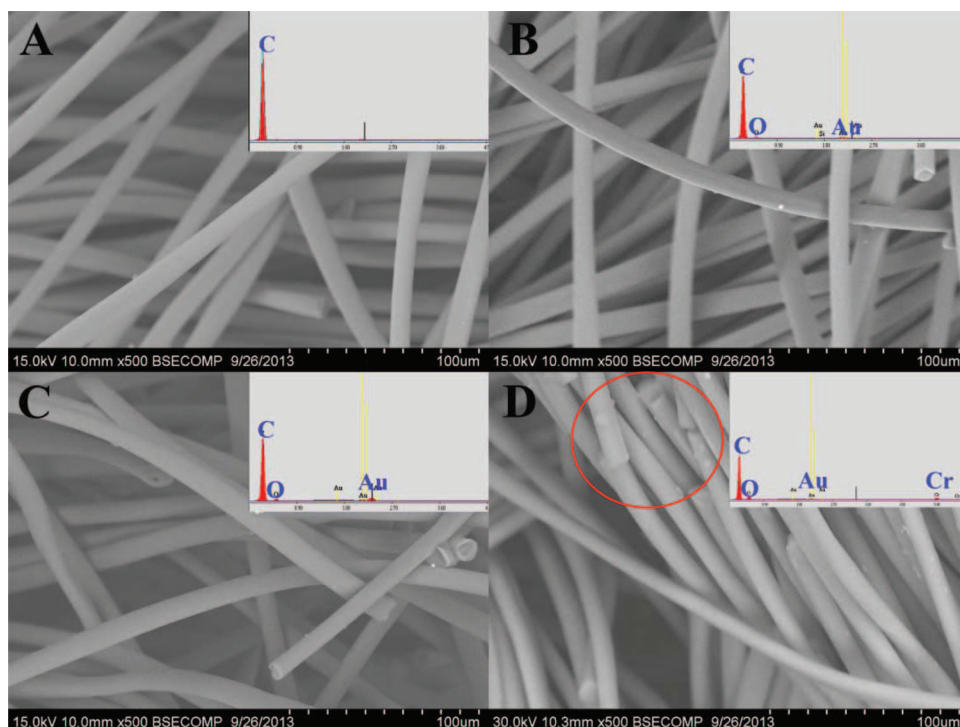
Figure 1. SEM microstructure and the EDS elemental analysis of (A) the as-received ACFs and the ACFs samples treated with (B) pH = 1.0, 1000 µg L^{-1} Cr(VI) solution, (C) pH = 7.0, 1000 µg L^{-1} Cr(VI) solution and (D) pH = 1.0, 2 g L^{-1} Cr(VI) solution. Top inset is the EDS spectra obtained from the SEM imaged area.
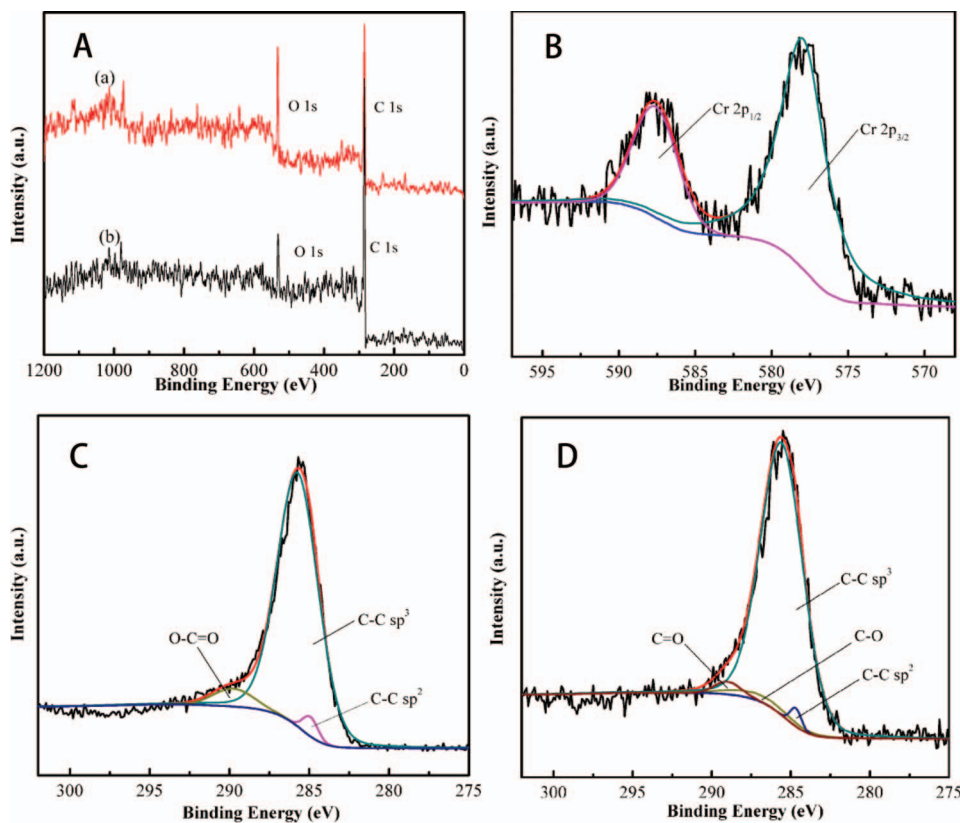
Figure 2. (A) XPS wide-scan survy spectra of (a) the as-received ACFs and (b) the ACFs sample treated with pH = 1.0 1000 µg L^{-1} Cr(VI) solution for 30 min; (B) deconvolution of high resolution Cr 2p XPS spectra of the ACFs treated with 2 g L^{-1} for 10 min; deconvolution of high resolution C 1s XPS spectrum of (C) the as-received ACFs and (D) the ACFs sample treated with pH = 1.0 1000 µg L^{-1} Cr(VI) solution for 30 min.

(1000 µg L^{-1}) for 30 min, the microstructure and diameter of these treated ACFs are almost the same as those of the as-received ACFs, Fig. 1B & 1C, indicating that the ACFs are very durable and have great potential for reusage. However, after treated in pH = 1.0 Cr(VI) solution with high concentrated Cr(VI) solution (2 g L^{-1}) for 30 min, the surface of carbon fibers becomes rough, Fig. 1D, indicating that the carbon fibers are etched, but the diameter of these ACFs is still uniform as the fresh ones.

From the EDS analysis, the oxygen functional groups have been introduced to the ACFs after treated with Cr(VI) solution, in order to further investigate what kinds of oxygen functional groups formed on the ACFs, XPS measurements of the as-received and treated ACFs samples were conducted. Fig. 2A shows the XPS wide-scan survey spectra of the ACFs and the ACFs treated with pH = 1.0, 1000 µg L^{-1} Cr(VI) solution. In the ACFs sample, the main C 1s binding energy peak at around 285 eV and O 1s binding energy peak at around 533 eV[36] are observed. Compared with the as-received ACFs, the ratio of the intensity of the elemental oxygen to the intensity of the elemental carbon on the surface of the treated ACFs increases. And according to quantity report from XPS, the mass concentrations of C 1s, O 1s and Cr 2p of the treated ACFs are 74.17, 21.98 and 3.84%, respectively, while those of the as-received ACFs are 97.58, 2.42 and 0%, respectively. The increased amount of oxygen in the treated ACFs is attributed to the formation of oxygen functional groups on the ACFs, which agrees well with the EDS analysis.

The deconvolution of the high resolution C 1s XPS spectra of the as-received ACFs and the ACFs treated with pH = 1.0, 1000 µg L^{-1} Cr(VI) solution are shown in Fig. 2C & 2D, respectively. The C 1s peak of the as-received ACFs in Fig. 2C is smoothly deconvoluted into three fitting curves with peaks at 284.7, 285.3 and 290.5 eV, which can be assigned to the sp^2-bonded C-C, the sp^3-bonded C-C and the O-C=O group, respectively.[37] However, for the treated ACFs in Fig. 2D, new peaks attributed to the C=O and C-O group appear at around 289.0 and 286.6 eV, respectively.[38–40] This suggests that the carbon in the ACFs has been oxidized (C-H → C-OH→ C-O and C=O) after treated with pH = 1.0, 1000 µg L^{-1} Cr(VI) solution.[41]

The Cr element valence state after adsorption is also examined by XPS measurement. Fig. 2A shows the Cr 2p spectrum of the ACFs sample after treated with pH = 1.0 solution with a concentration of 2.0 g L^{-1} for 10 min at room temperature. In the low Cr(VI) concentration solution, such as 1000 µg L^{-1}, the Cr element cannot be detected by XPS measurement, thus the high Cr(VI) concentration of 2 g L^{-1} is chosen for the Cr element valence state evaluation. Generally, for the Cr 2p XPS spectrum, the characteristic binding energy peaks for the Cr(VI) are at 580.0–580.5 and 589.0–590.0 eV and the Cr(III) characteristic binding energy peaks at 577.0–578.0 eV from the Cr 2p$_{3/2}$ orbital and 586.0–588.0 eV from the Cr 2p$_{1/2}$ orbital.[42,43] The observed binding energy peaks of Cr 2p located at around 577.5 and 588.2 eV in Fig. 2B, characteristic of Cr(III) confirm that the adsorbed Cr is in the Cr(III) form on the ACFs.[42] The presence of Cr(III) on the ACFs implies that the Cr(VI) ions have been reduced to Cr(III) ions. This indicates that the Cr(VI) adsorption process is occurred through a combined redox reaction, in which the toxic Cr(VI) is reduced to non-toxic Cr(III) and absorbed on the ACFs. On the other hand, the ACFs are oxidized as confirmed by C1s XPS spectra (Fig. 2C & 2D).

To further confirm that Cr(III) have been adsorbed onto the ACFs after redox reaction, an ammonium persulfate (APS) oxidant was used to oxidize the possible Cr(III) to Cr(VI) to trace the fate of Cr. After excessive amount of ACFs (50.0 mg) treated with 50.0 mL Cr(VI) solution (pH = 1.0 1000 µg L^{-1}) for 30 min, the ACFs were taken out from the solution, no Cr(VI) ion was detected by the colorimetric method in the solution implying a complete removal of Cr(VI). Excessive 0.1 mol/L APS aqueous solution as oxidizing agent was added to the above solution,[44] and the mixed solution was heated to 90°C for 10 min, the colorimetric analysis confirmed the absence of Cr(VI) in the solution. Furthermore, the above treated ACFs had been treated following the same as the treated solution, the ACFs were added to excessive 0.1 mol/L APS solution, then heated to 90°C for 10 min. UV-vis results show that Cr(VI) was detected in the latter APS treated ACFs solution, suggesting that the Cr(VI) was reduced to Cr(III) and Cr(III) was completely adsorbed on the ACFs. This
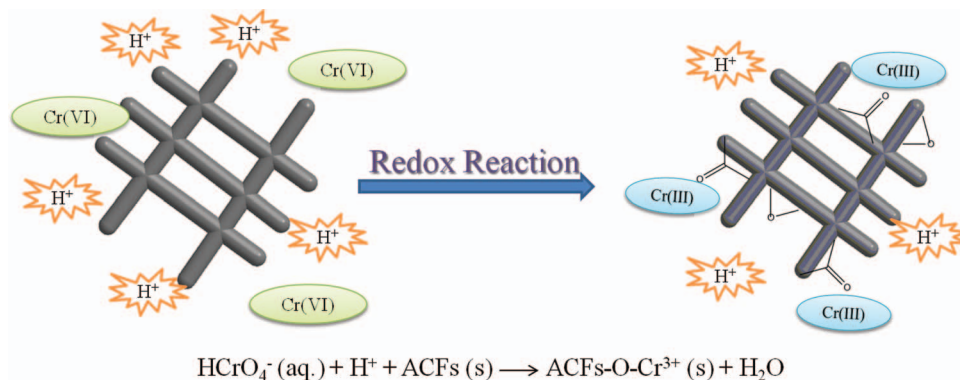
Scheme 1. The interaction between the ACFs and Cr(VI).

result agrees with the XPS and EDS analysis. Also, Cr(III) in aqueous solution exists as $[Cr(H_2O)_6]^{3+}$, the adsorption of Cr(III) on the surface of ACFs occurs through the electrostatic attraction between the carbon-oxygen functional groups and Cr(III).[45]

In summary, the adsorption of Cr(VI) using ACFs as absorbent is through a redox reaction, the Cr(VI) is reduced to Cr(III) that adsorbed on the ACFs, and the ACFs are oxidized. The C=O and C-O groups are formed on the ACFs after treated in pH = 1.0 Cr(VI) solution. The synergistic interaction between Cr(VI) and the ACFs in the pH = 1.0 solution is shown in Scheme 1.

Effects of pH value of Cr(VI) solution on the ACFs.— The solution pH is an important parameter influencing the heavy metal removal process, including Cr(VI) removal.[16,46] The pH dependent heavy metal removal is related not only to the metal chemistry in the solution but also to the type of the adsorbents. Fig. 3A shows the Cr(VI) removal percentage for the initial concentration of $1000\,\mu g\,L^{-1}$ Cr(VI) solution (50.0 mL) with different pH values after treated with 40.0 mg ACFs for 30 min at room temperature. The Cr(VI) removal percentage by the ACFs is observed to depend on the pH value. The obvious decrease

of the Cr(VI) removal percentage is observed from pH = 1.0 to 10.0, whereas an almost complete removal is found in pH = 1.0 solution. These results indicate that when pH > 7, Cr(VI) removal by the ACFs is not efficient (<35.7%).

In the aqueous Cr(VI) solution, dichromate ions $(Cr_2O_7^{2-})$ are in equilibrium with chromate ions (CrO_4^{2}), Equation 2:[47]

$$Cr_2O_7^{2-} + H_2O \leftrightarrow 2CrO_4^{2-} + 2H^+ \qquad [2]$$
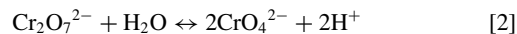
which is a dynamic equilibrium and sensitive to the pH value of solution. In the acidic solution, the equilibrium shifts to the left toward dichromate ions, $Cr_2O_7^{2-}$ is the dominating species. On the contrary, in the basic solutions, CrO_4^{2-} is the only chromate in the solution.[47]

Typically, in acidic solution, $Cr_2O_7^{2-}$ turns to $HCrO_4^-$, which exhibits a very high redox potential (1.33 V) and thus can be easily reduced to Cr(III), Equation 3:[48]

$$Cr_2O_7^{2-} + H_2O \rightarrow 2HCrO_4^-$$

$$[3]$$

$$HCrO_4^- + 7H^+ + 3e^- \rightarrow Cr(III) + 4H_2O \quad E_o = 1.33\,V$$
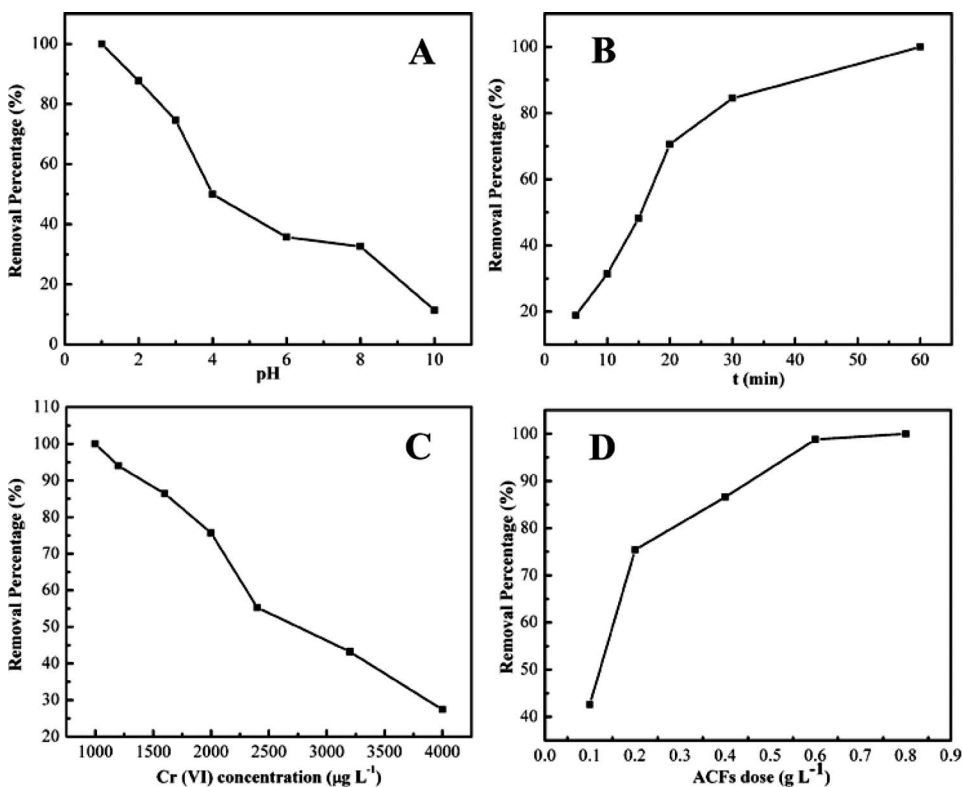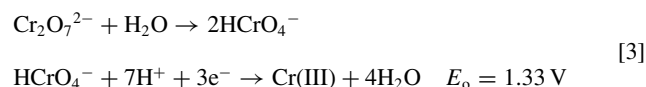
Figure 3. Cr(VI) removal percentage as a function of (A) pH value (50.0 mL $1000\,\mu g\,L^{-1}$ initial Cr(VI) concentration solution with 40.0 mg ACFs after 30 min treatment); (B) treatment time (80.0 mL pH = 1.0, $1000\,\mu g\,L^{-1}$ Cr(VI) solution with 50.0 mg ACFs; (C) initial Cr(VI) concentration (50.0 mL pH = 1.0 Cr(VI) solution with 40.0 mg ACFs after 30 min treatment); (D) ACFs dose (50.0 mL pH = 1.0, $1000\,\mu g\,L^{-1}$ initial Cr(VI) concentration solution after 30 min treatment).
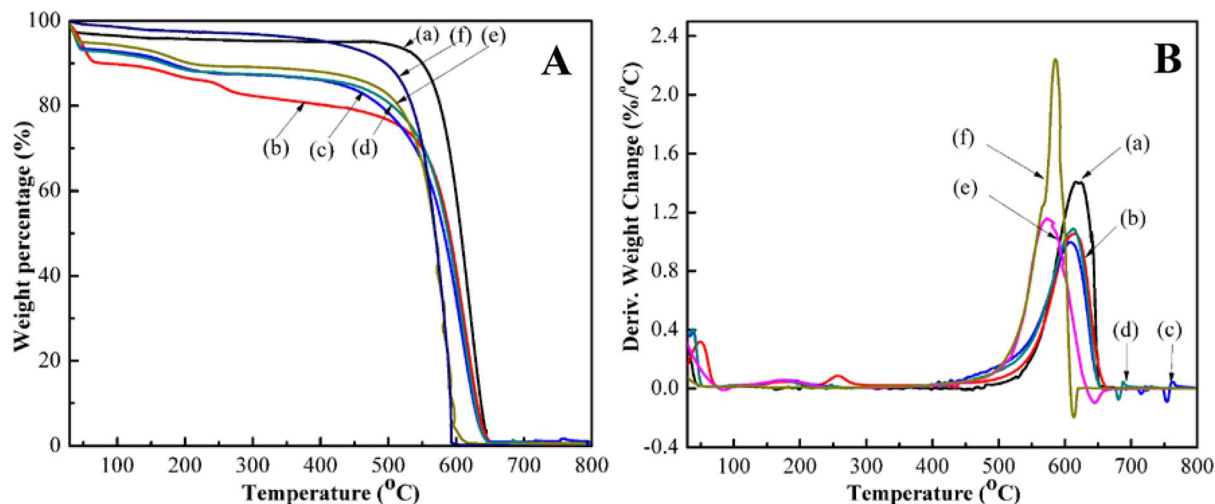
Figure 4. (A) TGA curves of (a) the as-received ACFs and the ACFs samples treated with the Cr(VI) solution of a pH value of (b) 1.0, (c) 2.0, (d) 4.0, (e) 8.0 and (f) 10.0 for 30 min; and (B) DTG curves of (a) the as-received ACFs and the ACFs samples treated with the Cr(VI) solution of a pH value of (a) 1.0, (c) 2.0, (d) 4.0, (e) 8.0 and (f) 10.0 for 30 min.

However, in alkaline solution, the CrO_4^{2-} is the dominating ions in solution. The oxidation ability of CrO_4^{2-} is weaker than that of $Cr_2O_7^{2-}$ ion due to the low redox potential (-0.13 V) and the Cr(III) hydroxide precipitation is produced:

$$CrO_4^{2-} + 4H_2O + 3e^- \rightarrow Cr(OH)_3 + 5OH^- \quad E_o = -0.13 \text{ V} \quad [4]$$
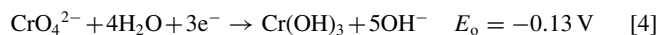
To better understand the interactions between ACFs and Cr(VI) in the solution with different pH values, the TGA and Raman spectra of the ACFs and the ACFs samples treated with solutions with different pH value were conducted, Fig. 4 & 5. In the TGA curves, Fig. 4, the as-received ACFs exhibit two-stage weight loss before $100°C$ and from 500 to $650°C$, which are due to the weight loss of the physically adsorbed water and the thermal degradation of the hexagonal carbon from the ACFs, respectively.[49] The TGA curves of the ACFs samples treated with Cr(VI) solutions with different pH value have different thermal degradation profile from the as-received ACFs. Another weight loss from 110 to $200°C$ is observed in the ACFs sample treated with pH $\geq$ 1.0 Cr(VI) solution. This is attributed to the degradation of the C-O groups.[50,51] However, for the ACFs sample treated with

pH = 1.0 Cr(VI) solution, except for the weight loss of C-O group, additional weight loss and endothermic peak at around $220-300°C$ are observed in Fig. 4A & 4B, respectively, arising from the degradation of C=O group.[52] However, the TGA curve of the ACFs sample treated with high pH value of 10.0 only has two weight loss regions similar to the as-received ACFs, due to the weaker oxidation ability of Cr(VI) ion in high pH Cr(VI) solution. The ACFs samples treated with Cr(VI) solutions with different pH value have different thermal stability. The degradation temperature (defined as 10% weight loss of total weight subtracting the weight of physically absorbed water) is 560, 389, 427, 468 and $491°C$ for the as-received ACFs sample and the ACFs samples treated with pH = 1.0, 2.0, 4.0, 8.0 and 10.0 Cr(VI) solutions, respectively. The thermal stability of ACFs samples increases with increasing the pH value of Cr(VI) solution due to the higher degree of carbon oxidation in low pH solution arising from the much higher redox potential of Cr(VI) in acid solutions than that in alkaline solutions.[53]

In order to evaluate the degree of surface structural change of the ACFs during the interactions with Cr(VI), the Raman spectra of the ACFs treated with Cr(VI) solution (1000 μg L^{-1}) of different pH values for 30 min were obtained, Fig. 5. Generally, the Raman spectra, well known as an important way to obtain the structural characterization of graphitic materials, can provide valuable information about the defects, stacking of the graphene layers and the crystallite size to the hexagonal axis, which are normally not detectable in other analytical tools.[54] Carbon fibers are a graphite-like material, the disorder-induced D-band at around 1293 cm^{-1} indicates the presence of the defects on the fiber arising from the sp^3 C-C bonds formed in the surface treatment. The tangential mode (E_{2g} symmetry, graphite mode) G-band appearing at 1585 cm^{-1} is due to the sp^2 C=C bond stretching vibrations.[55] The intensity of D-band and the intensity of G-band are found to continuously increase, Fig. 5, and the R value (defined as I_D/I_G, the integrated intensity of the D band divided by the integrated intensity of the G band) is continuously increased with increasing pH value. This result suggests that certain amount of structural disorder is generated by the preferential attack of oxygen species on the surface of the fibers[37,56] and the disorder is more pronounced in acidic solutions than that in alkaline solutions, which is consistent with the analysis of TGA.
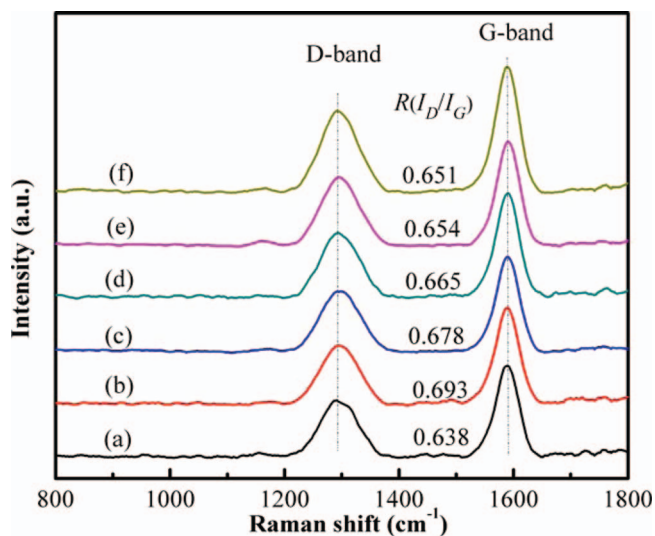
Figure 5. Raman spectra of (a) the as-received ACFs and the ACFs samples treated with the Cr(VI) solution of a pH value of (b) 1.0, (c) 2.0, (d) 4.0, (e) 8.0 and (f) 10.0 for 30 min.

Effects of treatment time and the initial Cr(VI) concentration on the ACFs.— Fig. 3B shows the Cr(VI) removal percentage from the initial concentration of 1000 μg L^{-1} Cr(VI) solution (80.0 mL) over different treatment periods ranging from 5 from 60 min. The amount
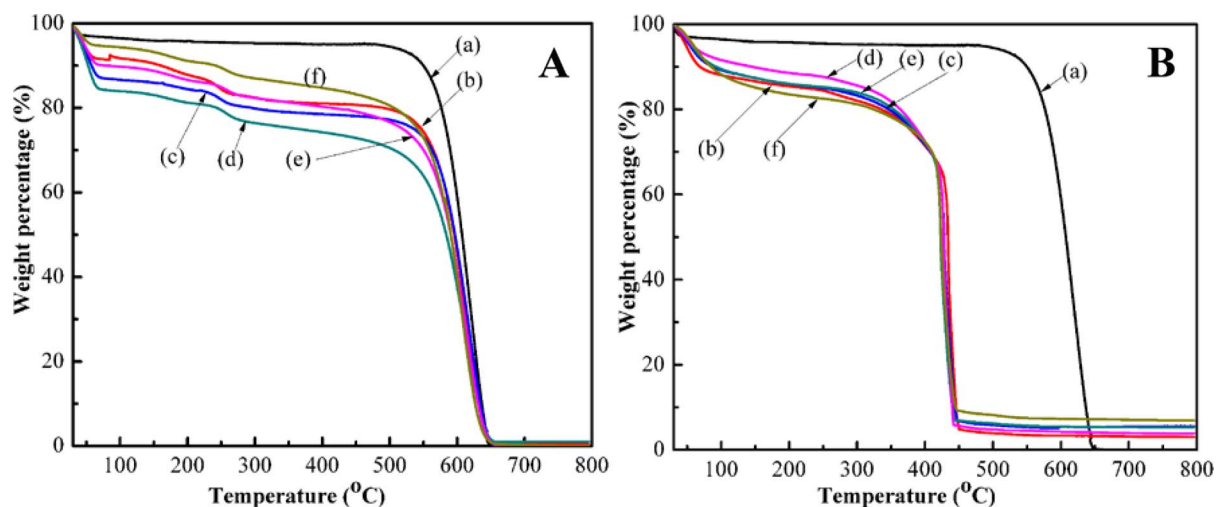
Figure 6. (A) TGA curves of (a) the as-received ACFs and the ACFs samples treated with pH = 1.0, 1000 μg L^{-1} Cr(VI) solution with a treatment time of (b) 5, (c) 10, (d) 20, (e) 30 and (f) 60 min; (B) TGA curves of (a) the as-received ACFs and the ACFs samples treated with pH = 1.0 2 g L^{-1} Cr(VI) solution with a treatment time of (b) 5, (c) 10, (d) 20, (e) 30 and (f) 60 min.

of Cr(VI) in the 80 mL 1000 μg L^{-1} Cr(VI) solution with pH = 1.0 can be effectively and completely removed by 50.0 mg ACFs in 60 min.

Fig. 3C shows the effect of initial Cr(VI) concentration on the Cr(VI) removal in the pH = 1.0 Cr(VI) solution over a treatment period of 30 min. The ACFs with a weight of 40.0 mg are observed to be able to treat 50.0 mL pH = 1.0 Cr(VI) solution with a 100% removal, while only around 27.4% of the Cr(VI) is removed with increasing Cr(VI) concentration to 4000 μg L^{-1}. The ACFs have a very large specific surface area (1500 m^2 g^{-1}) and large active sites for reacting with the Cr(VI). Although the removal percentage is observed to decrease with increasing the initial Cr(VI) concentration since these sites become saturated with increasing the Cr(VI) concentration and cannot accommodate excessive Cr(VI) at higher Cr(VI) concentration.[57]

The TGA analysis is also used to investigate the structural change of the ACFs samples treated with pH = 1.0 Cr(VI) solution over different period time ranging from 5 to 60 min for the initial Cr(VI) concentration of 1000 μg L^{-1}. The results are shown in Fig. 6A, compared to the weight loss curve of the as-received ACFs, the TGA curves of the ACFs sample treated with 1000 μg L^{-1} pH = 1.0 Cr(VI) solution, have two additional weight loss regions at around 110–200 and 220–300°C, which are attributed to the degradation of C-O and C=O groups, respectively, as justified by XPS studies, Fig. 1C. In addition, the thermal stability of the ACFs sample after treated with pH = 1.0 Cr(VI) solution decreases because of the formation of C-O and C=O groups on the surface of the ACFs. However, for the ACFs samples treated with pH = 1.0, 2 g L^{-1} Cr(VI) solution over different period time ranging from 5 to 60 min, the thermal stability of all the ACFs samples decreases dramatically, Fig. 6B, the ACFs samples begin to degrade at around 100°C and are completely degraded before 450°C. This is attributed to strong oxidation of high concentrated Cr(VI) solution, and more and more oxygen functional groups are formed on the ACFs, as verified by prior EDS and XPS analysis.

The Raman spectra of the as-received ACFs and the ACFs samples treated with pH = 1.0, 2 g L^{-1} Cr(VI) solution with different period time are shown in Fig. 7, the width of D band and G band of the treated ACFs with treatment time from 5 to 60 min, becomes broadened, D band peak shifts from 1293 to 1300 cm^{-1}, and the *R* value is continuously increased, indicating that the disorder of the ACFs increases with increasing the treatment time, the disorder of the ACFs treated with concentrated Cr(VI) solution is more serious than that with the 1000 μg L^{-1} Cr(VI) solution, and more oxygen functional groups are introduced on the surface of the ACFs.

Effects of the ACFs dose on the ACFs.— The effects of the ACFs dose on the Cr(VI) removal percentage were tested over the same 30 min treatment, Fig. 1D. The removal percentage is observed to increase with increasing the ACFs concentration, which is due to the more available active sites for trapping Cr(VI).[7] At low dose (<0.6 g L^{-1}), the Cr(VI) removal percentage increases sharply, when the dose increases to 0.6 g L^{-1}, the Cr(VI) in the solution is almost removed 100%. The dose of 0.8 g L^{-1} can remove 50.0 mL solution contaminated with 1000 μg L^{-1} initial Cr(VI) concentration, indicating that the ACFs have a good removal performance for Cr(VI) contaminated solution.

Adsorption kinetics.— The kinetics of the adsorption describing the Cr(VI) uptake rate is one of the important characteristics, which controls the residence time of adsorbate uptake at the solid-liquid interface. In the present study, the kinetics of Cr(VI) removal was carried out to understand the adsorption behavior of the ACFs. Pseudo-first-order,[58] pseudo-second-order,[59] Elovich[60,61] and intra-particle diffusion[62] kinetic models are investigated and comparatively tested for the ACFs adsorption behavior. The correlation coefficient
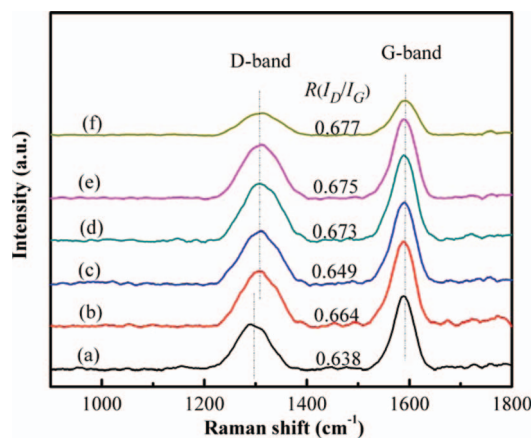
Figure 7. Raman spectra of (a) the as-received ACFs and the ACFs samples treated with pH = 1.0, 2 g L^{-1} Cr(VI) solution with a treatment time of (b) 5, (c) 10, (d) 20, (e) 30 and (f) 60 min.

Table I. The parameters obtained from different kinetic models.

Models	Equation[a]	Parameters		R^2
Pseudo-first-order	$\log(q_e - q_t) = \log q_e - \dfrac{k_1}{2.303}t$	k_1 (min^{-1}) 0.0872	q_e (mg g^{-1}) 1.578	0.961
Pseudo-second-order	$\dfrac{t}{q_t} = \dfrac{1}{k_{ad}q_e^2} + \dfrac{t}{q_e}$	k_{ad} (g mg^{-1} min^{-1}) 0.0029	q_e (mg g^{-1}) 3.944	0.444
Elovich	$q_t = \dfrac{1}{\beta}\ln(\alpha\beta) + \dfrac{1}{\beta}\ln t$	α (mg g^{-1} min^{-1}) 1.42×10^{-13}	β (g mg^{-1}) 16.97	0.858
Weber-Morris intraparticle diffusion	$q_t = k_{dif}t^{0.5} + C$	k_{dif} (mg g^{-1} min$^{-0.5}$) -0.3635	C (mg g^{-1}) 0.252	0.958

[a]q_t is the solid-phase loading of Cr(VI) in the adsorbent at a time t, q_e is the adsorption capacity at equilibrium, k_1 is the rate constant of pseudo-first-order adsorption. In pseudo-second-order model, k_{ad} is the rate constant of adsorption and h is the initial adsorption rate at t approaching zero, $h = k_{ad}q_e^2$. α and β represent the initial adsorption rate and desorption constant in the Enovich model. k_{dif} indicates the intraparticle diffusion rate constant and C provides information about the thickness of the boundary layer.

(R^2, close or equal to 1) is introduced to evaluate the suitability of different models, the higher R^2 value indicates a more applicable model to the kinetic of Cr(VI) adsorption.

The fitting results obtained from different models are summarized in Table I. With the highest correlation coefficient of R^2 = 0.961, pseudo-first-order model provides the best correlation for the adsorption of Cr(VI) on the ACFs. The correlation coefficients for the pseudo-second-order, Elovich and intraparticle diffusion models are 0.444, 0.858 and 0.958, respectively, indicating that these models are less suitable for describing the Cr(VI) adsorption on ACFs. The rate constant of pseudo-first-order k_1 of 0.0872 min^{-1} is great than the reported wool (0.0396 min^{-1}),[63] eucalyptus bark (0.0198 min^{-1})[64] and D354 anion-exchange resin (0.0670 min^{-1}).[65]

Adsorption isotherm models.— The adsorption isotherm models are widely used to describe the relation between the equilibrium concentration and adsorption capacity at a constant temperature. Langmuir,[66] Freundlich[67] and Temkin models[68] were used to process the experimental data.

The Langmuir isotherm model[13] assumes that adsorption is essentially monolayer coverage, all the sites are the same and it neglects the interaction among the adsorbed molecules. The Freundlich isotherm model[69] supposes the surface of adsorbent is heterogeneous, the heat of adsorption on the surface is a nonuniform distribution and the adsorption is a multilayer coverage. Temkin isotherm model[70] is based on the assumptions: (a) the behavior of adsorption is heterogeneous systems; and (b) the adsorption heat linearly decreases with increasing adsorption quantity, and the adsorption binding energy is distributed uniformly. The equilibrium adsorption experiment was investigated by using ACFs (40.0 mg) to treat Cr(VI) solution (50.0 mL, pH = 1.0) with Cr(VI) concentration varying from 1000 to 4000 μg L^{-1} for 60 min, the parameters calculated from these three isotherm models are listed in Table II. On the basis of the correlation coefficient values, it can be seen that the Langmuir isotherm model fits best to the experimental data than the Freundlich and the Temkin isotherm

model, with the maximum adsorption capacity of 5.59 mg g^{-1}, which is much higher than the previously reported values of biomass materials, such as coconut shell charcoal (4.72 mg g^{-1}),[71] coconut tree (3.46 mg g^{-1})[72] and agricultural waste biomass (0.82 mg g^{-1}).[73]

Regeneration of ACFs.— From a practical point of view, the recycling and reuse of the adsorbent is an economic necessity. To evaluate the reusability of ACFs, 0.1 mol L^{-1} NaOH solution was selected to be a desorption agent in the Cr(VI) desorption experiment. The saturated ACFs (40 mg) were ultrasonically treated with 10 mL 0.1 mol L^{-1} NaOH solution over a period time of 10 min. The adsorption-desorption cycles were repeated seven times, the removal percentage of Cr(VI) in every run is shown in Fig. 8. The removal percentage of Cr(VI) remains 100% for the fourth regeneration cycle, then decreases slowly. As compared to the first adsorption, the
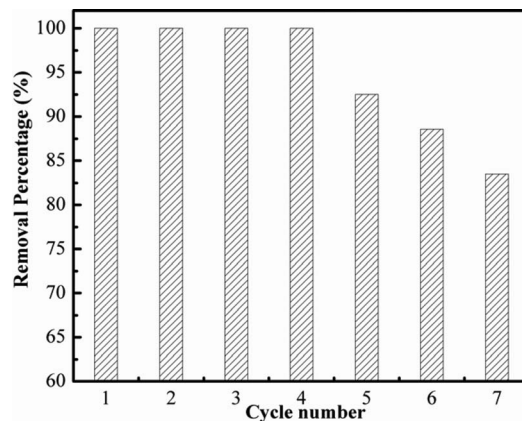
Figure 8. Regeneration studies of ACFs in the removal of Cr(VI) (adsorption: 50 mL, pH = 1.0, 1000 μg L^{-1} Cr(VI) solution, 40 mg ACFs, 30 min; desorption: 10 mL, 0.1 mol L^{-1} NaOH solution, 10 min).

Table II. Equilibrium parameters for Cr(VI) adsorption.

Models	Equation[a]	Parameters		R^2
Langmuir isotherm	$\dfrac{C_e}{q_e} = \dfrac{1}{bq_{max}} + \dfrac{C_e}{q_{max}}$	q_{max} (mg g^{-1}) 5.593	b (L mg^{-1}) 8.86×10^{-3}	0.923
Freundlich isotherm	$\log q_e = \log k_f + \dfrac{1}{n}\log C_e$	k_f (mg g^{-1}) 0.635	n 2.508	0.910
Temkin isotherm	$q_e = \dfrac{RT}{b_T}\ln A_T + \dfrac{RT}{b_T}\ln C_e$	A_T (L mg^{-1}) 1.176	b_T (J mol^{-1}) 837.26	0.844

[a]C_e and q_e is the concentration and adsorption capacity at equilibrium, respectively, q_{max} is the monolayer adsorbent capacity, b is the energy constant of adsorption. k_f is the Freundlich capacity factor and n is the Freundlich's intensity factor, the value of n in range of 1–10 denotes favorable adsorption. A_T and B_T are the Temkin constants. R is the universal gas constant 8.314 J mol^{-1} K^{-1}, and T is the absolute temperature.
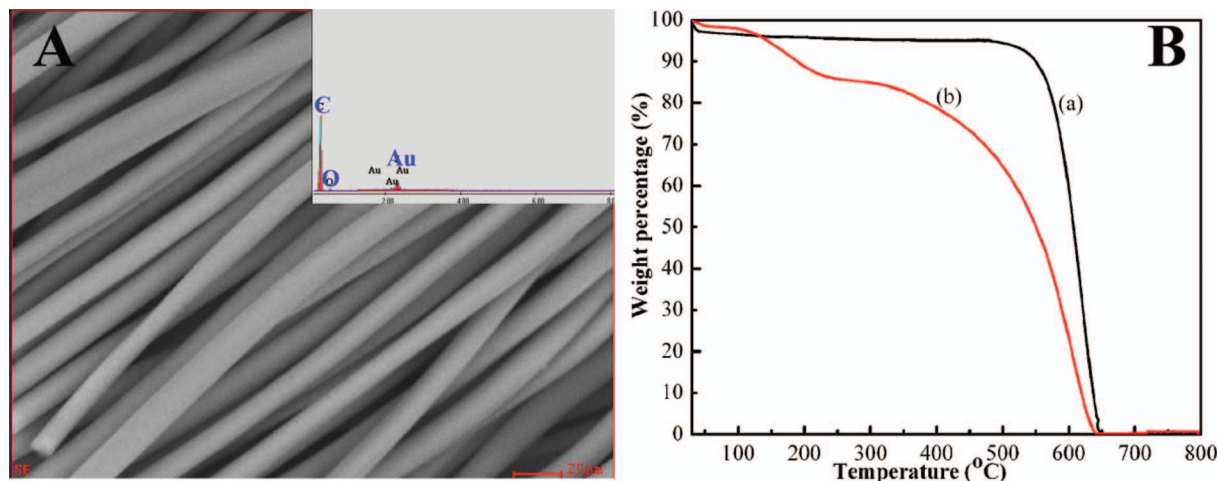
Figure 9. (A) SEM microstructure of the ACFs sample after the 7th desorption and (B) the TGA curves of (a) the as-received ACFs and (b) the ACFs sample after the 7th desorption. Top inset is the EDS spectrum of the ACFs sample after the 7th desorption obtained from the SEM imaged area.

removal percentage of Cr(VI) at the seventh cycle is decreased by about 16.5% to a value of 83.5%, indicating that the ACFs have a good regeneration and reusability for many times. The SEM-EDS and TGA characterization of the ACFs sample after the 7th desorption were conducted to investigate the reasons for the decreased Cr(VI) removal behavior, the results are shown in Fig. 9. In Fig. 9A, the SEM image of the ACFs after the 7th desorption is almost the same as the fresh ones, Fig. 1A, and the surface of these ACFs is still smooth and the diameter is uniform, thus there is no obvious damage or etch on the ACFs after the 7th desorption. Though there is no obvious damage from the SEM image, some differences between the as-received ACFs and the ACFs sample after the 7th adsorption are observed in the TGA curves, Fig. 9B. The TGA curves of the ACFs sample after the 7th desorption has three weight loss regions, The first one is assigned to the physically absorbed water, the second one at around 100–200°C is the degradation of C-O group as discussed in the Fig. 4. The last one from 200 to 650°C is the degradation of the C=O group and the hexagonal carbon from the ACFs. Compared to the fresh ACFs, oxygen functional groups are formed on the surface of the ACFs and accumulated on the ACFs, which cannot be removed by the desorption process. Thus, the decreased chromium removal behavior of the ACFs is caused by the accumulation of C-O and C=O groups on the ACFs, which cannot be irreversible removed by 0.1 mol L^{-1} NaOH solution.

Conclusions

The synergistic interactions between the ACFs and the toxic Cr(VI) solutions with different pH values were investigated. FT-IR, TGA, SEM and XPS analyzes show that the Cr(VI) in the solution with different pH values has different effects on the ACFs. For the pH = 1.0 Cr(VI) solution, the as-received ACFs are strongly oxidized by Cr(VI) solution with the formation of the C-O and C=O functional groups on the ACFs. For the pH > 2.0 Cr(VI) solutions, the Cr(VI) removal percentage decreases dramatically and some oxidation of the ACFs is also observed, which is not intense as that in the pH = 1.0 solution. The kinetics for different Cr(VI) removal models shows that in the pH = 1.0 solution, the redox reaction dominates the Cr(VI) removal process and follows a pseudo-first-order behavior. The Langmiur, Freundlich and Temkin isotherm models are used to study the adsorption behavior; Langmuir isotherm model fits best to the experimental data. The recycle of ACFs has been run for 7 times and shown good regeneration.

References

1. S. Kalidhasan, M. Ganesh, S. Sricharan, and N. Rajesh, *J. Hazard. Mater.*, **165**, 886 (2009).
2. J. R. Rao, P. Thanikaivelan, K. J. Sreeram, and B. U. Nair, *Environ. Sci. Technol.*, **36**, 1372 (2002).
3. S. Vasudevan, G. Sozhan, S. Mohan, R. Balaji, P. Malathy, and S. Pushpavanam, *Ind. Eng. Chem. Res.*, **46**, 2898 (2007).
4. J. Samuel, M. L. Paul, M. Pulimi, M. J. Nirmala, N. Chandrasekaran, and A. Mukherjee, *Ind. Eng. Chem. Res.*, **51**, 3740 (2012).
5. D. Zhang, S. Wei, C. Kaila, X. Su, J. Wu, A. B. Karki, D. P. Young, and Z. Guo, *Nanoscale.*, **2**, 917 (2010).
6. B. Dhal, H. N. Thatoi, N. N. Das, and B. D. Pandey, *J. Hazard. Mater.*, **250–251**, 272 (2013).
7. J. Hu, C. Chen, X. Zhu, and X. Wang, *J. Hazard. Mater.*, **162**, 1542 (2009).
8. K. H. Cheung and J.-D. Gu, *Int. Biodeterior. Biodegrad.*, **59**, 8 (2007).
9. L. Monser and N. Adhoum, *Sep. Purif. Technol.*, **26**, 137 (2002).
10. N. Kongsricharoern and C. Polprasert, *Water Sci. Technol.*, **31**, 109 (1995).
11. C. Altman and E. L. King, *J. Am. Chem. Soc.*, **83**, 2825 (1961).
12. Y. C. Sharma, B. Singh, A. Agrawal, and C. H. Weng, *J. Hazard. Mater.*, **151**, 789 (2008).
13. A. S. K. Kumar, S. Kalidhasan, V. Rajesh, and N. Rajesh, *Ind. Eng. Chem. Res.*, **51**, 58 (2011).
14. N. N. Fathima, R. Aravindhan, J. R. Rao, and B. U. Nair, *Environ. Sci. Technol.*, **39**, 2804 (2005).
15. J. Zhu, S. Wei, H. Gu, S. B. Rapole, Q. Wang, Z. Luo, N. Haldolaarachchige, D. P. Young, and Z. Guo, *Environ. Sci. Technol.*, **46**, 977 (2011).
16. R. Aravindhan, B. Madhan, J. R. Rao, B. U. Nair, and T. Ramasami, *Environ. Sci. Technol.*, **38**, 300 (2003).
17. D. Kratochvil, P. Pimentel, and B. Volesky, *Environ. Sci. Technol.*, **32**, 2693 (1998).
18. R. Kumar, M. O. Ansari, and M. A. Barakat, *Chem. Eng. J.*, **228**, 748 (2013).
19. T. Otowa, Y. Nojima, and T. Miyazaki, *Carbon*, **35**, 1315 (1997).
20. E. C. Bernardo, R. Egashira, and J. Kawasaki, *Carbon*, **35**, 1217 (1997).
21. K. A. Halhouli, N. A. Darwish, and N. M. Al-Dhoon, *Sep. Sci. Technol.*, **30**, 3313 (1995).
22. G. McKay, M. J. Bino, and A. R. Altamemi, *Water Res.*, **19**, 491 (1985).
23. J. Przepiórski, S. Yoshida, and A. Oya, *Carbon*, **37**, 1881 (1999).
24. L. Monser and N. Adhoum, *Sep. Purif. Technol.*, **26**, 137 (2002).
25. M. Pavageau, L. Le Coq, J. Mabit, and C. Solliec, *Chem. Eng. Sci.*, **55**, 2699 (2000).
26. D. Mohan, K. P. Singh, and V. K. Singh, *J. Hazard. Mater.*, **152**, 1045 (2008).
27. M. A. A. Zaini, R. Okayama, and M. Machida, *J. Hazard. Mater.*, **170**, 1119 (2009).
28. D. Mohan, K. P. Singh, and V. K. Singh, *J. Hazard. Mater.*, **152**, 1045 (2008).
29. M. Uysal and I. Ar, *J. Hazard. Mater.*, **149**, 482 (2007).
30. V. K. Gupta and A. Rastogi, *J. Hazard. Mater.*, **154**, 347 (2008).
31. D. Sud, G. Mahajan, and M. P. Kaur, *Bioresour. Technol.*, **99**, 6017 (2008).

32. V. K. Gupta, S. Agarwal, and T. A. Saleh, *Water Res.*, **45**, 2207 (2011).
33. D. Mohan, K. P. Singh, and V. K. Singh, *J. Hazard. Mater.*, **135**, 280 (2006).
34. D. Mohan and C. U. Pittman Jr, *J. Hazard. Mater.*, **137**, 762 (2006).
35. M. Gardner and S. Comber, *Analyst*, **127**, 153 (2002).
36. L. Shao, Y. P. Bai, X. Huang, L. H. Meng, and J. Ma, *J. Appl. Polym. Sci.*, **113**, 1879 (2009).
37. Y. C. Jung, H. H. Kim, Y. A. Kim, J. H. Kim, J. W. Cho, M. Endo, and M. S. Dresselhaus, *Macromol.*, **43**, 6106 (2010).
38. W. H. Lee, S. J. Kim, W. J. Lee, J. G. Lee, R. C. Haddon, and P. J. Reucroft, *Appl. Surf. Sci.*, **181**, 121 (2001).
39. P. M. A. Sherwood, *J. Electron Spectrosc. and Relat. Phenom.*, **81**, 319 (1996).
40. D. Yang, A. Velamakanni, G. Bozoklu, S. Park, M. Stoller, R. D. Piner, S. Stankovich, I. Jung, D. A. Field, C. A. Ventrice Jr, and R. S. Ruoff, *Carbon*, **47**, 145 (2009).
41. Z. Yue, S. E. Bender, J. Wang, and J. Economy, *J. Hazard. Mater.*, **166**, 74 (2009).
42. D. Park, Y. S. Yun, and J. M. Park, *J. Colloid and Interface Sci.*, **317**, 54 (2008).
43. D. Duranoğlu, A. W. Trochimczuk, and U. Beker, *Chem. Eng. J.*, **187**, 193 (2012).
44. M. G. García, A. O. Acosta, and J. Marchese, *Desalination*, **318**, 88 (2013).
45. D. Aggarwal, M. Goyal, and R. C. Bansal, *Carbon*, **37**, 1989 (1999).
46. A. Mahapatra, B. G. Mishra, and G. Hota, *Ind. Eng. Chem. Res.*, **52**, 1554 (2012).
47. Y. Li, B. Gao, T. Wu, D. Sun, X. Li, B. Wang, and F. Lu, *Water Res.*, **43**, 3067 (2009).
48. P. A. Kumar, S. Chakraborty, and M. Ray, *Chem. Eng. J.*, **141**, 130 (2008).
49. A. C. Baudouin, J. Devaux, and C. Bailly, *Polym.*, **51**, 1341 (2010).
50. Carlos M. García Santander, Sandra M. Gómez Rueda, Nívea de Lima da Silva, Celso L. de Camargo, T. G. Kieckbusch, and M. R. Wolf Maciel, *Fuel*, **92**, 158 (2012).
51. C. M. García Santander, S. M. Gómez Rueda, N. de Lima da Silva, C. L. de Camargo, T. G. Kieckbusch, and M. R. Wolf Maciel, *Fuel*, **92**, 158 (2012).
52. H. Gu, S. B. Rapole, Y. Huang, D. Cao, Z. Luo, S. Wei, and Z. Guo, *J. Mater. Chem. A*, **1**, 2011 (2013).
53. H. Gu, S. B. Rapole, J. Sharma, Y. Huang, D. Cao, H. A. Colorado, Z. Luo, N. Haldolaarachchige, D. P. Young, B. Walters, S. Wei, and Z. Guo, *RSC Adv.*, **2**, 11007 (2012).
54. M. A. Pimenta, G. Dresselhaus, M. S. Dresselhaus, L. G. Cancado, A. Jorio, and R. Saito, *PCCP*, **9**, 1276 (2007).
55. D. McIntosh, V. N. Khabashesku, and E. V. Barrera, *J. Phys. Chem. C*, **111**, 1592 (2007).
56. H. Gu, J. Guo, Q. He, Y. Jiang, Y.-D. Huang, N. Haldolaarachchige, Z. Luo, D. P. Young, S. Wei, and Z. Guo, *Nanoscale*, **6**, 181 (2014).
57. K. Pillay, E. M. Cukrowska, and N. J. Coville, *J. Hazard. Mater.*, **166**, 1067 (2009).
58. S. Lagergren, *Zur theorie der sogenannten adsorption gelöster stoffe, Kungliga Svenska Vetenskapsakademiens. Handlingar*, **24**, 1 (1898).
59. Y. S. Ho, G. McKay, D. A. J. Wase, and C. F. Forster, *Adsorpt. Sci. and Technol.*, **18**, 639 (2000).
60. R.-S. Juang and M.-L. Chen, *Ind. Eng. Chem. Res.*, **36**, 813 (1997).
61. D. L. Sparks, ed., *Kinetics of Reaction in Pure and Mixed Systems, in Soil Physical Chemistry*, CRC press, Boca Raton, (1986).
62. S. K. Srivastava, R. Tyagi, and N. Pant, *Water Res.*, **23**, 1161 (1989).
63. M. Dakiky, M. Khamis, A. Manassra, and M. Mer'eb, *Adv. Environ. Res.*, **6**, 533 (2002).
64. V. Sarin and K. K. Pant, *Bioresour. Technol.*, **97**, 15 (2006).
65. T. Shi, Z. Wang, Y. Liu, S. Jia, and D. Changming, *J. Hazard. Mater.*, **161**, 900 (2009).
66. L. Levankumar, V. Muthukumaran, and M. B. Gobinath, *J. Hazard. Mater.*, **161**, 709 (2009).
67. N. Passé-Coutrin, S. Altenor, and S. Gaspard, *J. Colloid Interface Sci.*, **332**, 515 (2009).
68. A. Mori and I. L. Maksimov, *J. Cryst. Growth*, **200**, 297 (1999).
69. Z. Yu, X. Zhang, and Y. Huang, *Ind. Eng. Chem. Res.*, **52**, 11956 (2013).
70. Y. Zhou, X. Hu, M. Zhang, X. Zhuo, and J. Niu, *Ind. Eng. Chem. Res.*, **52**, 876 (2012).
71. S. Babel and T. A. Kurniawan, *Chemosphere*, **54**, 951 (2004).
72. K. Selvi, S. Pattabhi, and K. Kadirvelu, *Bioresour. Technol.*, **80**, 87 (2001).
73. U. K. Garg, M. P. Kaur, V. K. Garg, and D. Sud, *J. Hazard. Mater.*, **140**, 60 (2007).